Journal of Structural Geology, Vol. 8, No. 7, pp. 819 to 830, 1986
Printed in Great Britain

0191-8141/86 $03.00 + 0.00

Some applications of the Mohr diagram for three-dimensional strain

SUSAN H. TREAGUS

Department of Geology, The University, Manchester, M13 9PL, U.K.

(*Received* 18 *July* 1985; *accepted in revised form* 9 *December* 1985)

Abstract—The Mohr diagram for strain is rarely used in its full form, as a representation of three-dimensional strain. Recent attention has focused on various uses of the Mohr circle to express two-dimensional strain tensors. This contribution redescribes the Mohr diagram for three-dimensional strain and illustrates some new applications. The Mohr diagram for any strain ellipsoid provides an immediate method for ellipsoid shape classification. However, its greatest new potential is considered to be in the representation of strain ellipses as sections of ellipsoids.

Any plane section of a strain ellipsoid can be plotted on the ellipsoid's Mohr diagram: it is here called a 'Mohr locus' because it is constructed as a locus of points representing the sheaf of lines which can be considered to define the plane. Mohr loci for sectional ellipses have a variety of forms, according to their orientation in the strain ellipsoid. Generally oblique sections are represented by loops bounded by the three principal circles. Their most leftward and rightward points are the plane's principal axes. Any Mohr locus can be transformed into a Mohr circle for the sectional ellipse.

Mohr diagrams with Mohr loci have considerable potential as a graphical method of deriving best-fit strain ellipsoids from natural strain data. This is illustrated in three examples.

THE MOHR DIAGRAM—HISTORICAL BACKGROUND

THE TERM *Mohr diagram* is used to encompass a family of graphical representations, either of stress or strain, which are characterized by circles, known as *Mohr circles*. The Mohr diagram for stress is most commonly used in the study of fracture, in which a *Mohr envelope* is constructed from successive Mohr circles at points of failure. In strain studies, a single Mohr circle is sometimes labelled a Mohr diagram: such circles may be used to illustrate two-dimensional strain tensors or as a practical method of strain determination. In modern structural geology, the Mohr diagram is restricted almost exclusively to two-dimensional analyses, either of stress or strain. This was not the case for the original Mohr diagram.

Mohr's original diagram (1882) was a representation of normal versus shear stress (σ, τ) for three-dimensional stress (Fig. 1). The diagram shows three principal stress circles (XY, YZ, XZ) and a method of plotting σ, τ for any plane in terms of angles of its pole to X and Z. The convention for measuring single angles is shown in Fig. 1(a), and double angles (the more usual present-day convention) in Fig. 1(b). Mohr's application of this diagram was mainly directed to practical mechanics and the representation of failure by means of the now well-known failure envelope (1882, 1900, 1905).

Nadai's (1931) textbook was probably the first explanation of Mohr's work in English. In a fuller account, Nadai (1950, chap. 10) described Mohr's representation of a state of stress as "Mohr's stress plane σ, τ" because the three-dimensional variation of σ and τ is represented in a plane.

Nadai (1950, pp. 124–130) first applied Mohr's stress representation to strain. Two graphs were introduced for quadratic elongation vs shear strain (Fig. 2). The diagram of λ vs γ (Nadai called γ unit shear), with angles measured in their unstrained state, is illustrated in Fig. 2(a). The three principal planes of the strain ellipsoid are represented by principal ellipses analogous to the circles in the stress diagram. However, Nadai recognized that a graph of reciprocal quadratic elongation λ' vs γ' ($\gamma' = \gamma/\lambda$), in terms of angles in the strained state, is identical in form with the Mohr stress diagram: the three principal planes of the strain ellipsoid are represented by three principal Mohr circles (Fig. 2b). The strain state for any other direction falls in the region bounded by the three circles.

It was probably Brace (1961) who first used the expression "Mohr diagram" in the geological literature for the representation of three-dimensional finite strain. He emphasized the distinctions between the two types of diagram (unstrained, Fig. 2a; strained, Fig. 2b) and examined their practical uses in structural geology. Ramsay (1967) expanded the usage of the Mohr diagram for strain in two ways. Firstly (1967, pp. 69–81) he illustrated the potential of Mohr circles for determining strain ellipses for particular sets of two-dimensional strain data. Secondly (1967, pp. 149–158) he illustrated how the diagram for three-dimensional reciprocal strain *sensu* Nadai might be used to compute strain. For five ellipsoid examples, Ramsay (fig. 4.21) thus derived strain contours which were represented on stereographic projections.

Despite the potential illustrated by Ramsay, Mohr diagrams for three-dimensional strain are not widely used. As a means of representing two-dimensional strain or deformation tensors, Mohr circles have enjoyed a recent surge of interest, however. For example, there

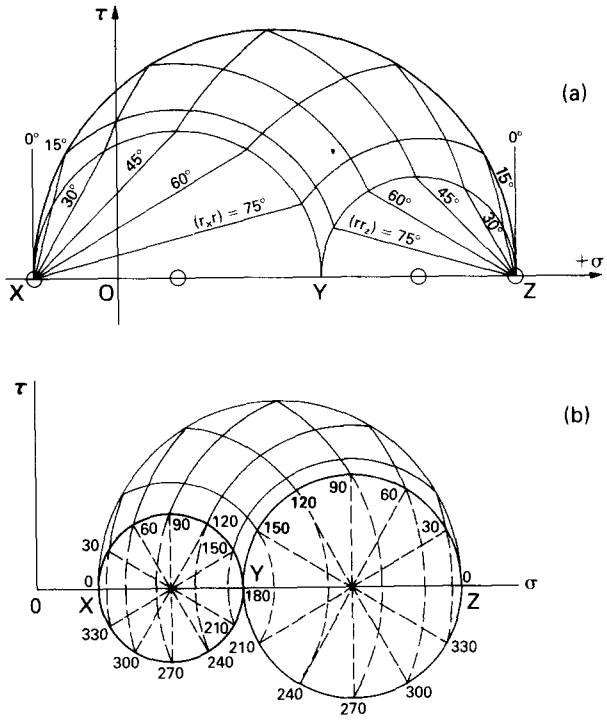

Fig. 1. Mohr's original (σ, τ) diagram, (a) in single-angle form (Mohr 1905, abb. 9) and (b) in double-angle form (*op. cit.*, abb. 20).

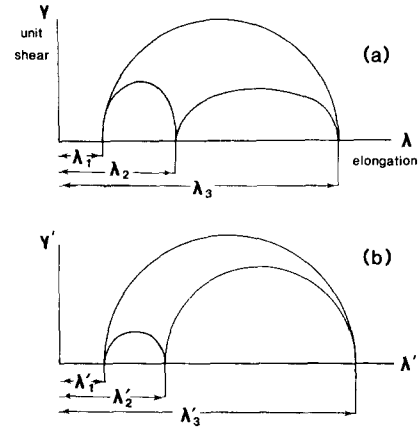

Fig. 2. The Nadai-Mohr type diagrams for strain (a) The elongation vs unit shear diagram, after Nadai (1950, fig. 12.9). (b) The reciprocal strain diagram (after Nadai 1950, fig. 12.10).

are off-axis Mohr circles for asymmetric second-order tensors (Means 1982, 1983, De Paor 1983, De Paor & Means 1984), poles to Mohr circles (Cutler & Elliott 1983, Allison 1984) and Mohr circles used to represent strain refraction (Means 1983, Treagus 1983). The following account returns to the Mohr diagram as a representation of three-dimensional strain and investigates some new applications in structural geology.

THE MOHR DIAGRAM FOR THREE-DIMENSIONAL STRAIN

The term *Mohr diagram* will be applied to the Mohr-Nadai representation of λ' vs γ' in three dimensions. Two-dimensional representations will be called *Mohr circles*. In practice, it is more convenient to represent three-dimensional strain states on a half Mohr diagram with three principal semi-circles (e.g. Nadai 1950, Jaeger 1956, Ramsay 1967), thus representing the value, but not the sign, of γ'.

A particular strain ellipsoid is represented by a three-circle Mohr diagram such as Fig. 2(b), on which the strain for any line occupies the field bounded by the three circles. Any line (L) is located stereographically in the manner shown in Fig. 3(a), by angles ϕ_1, ϕ_2 and ϕ_3 to λ'_1, λ'_2 and λ'_3, respectively. Three circular arcs are then drawn on the Mohr diagram; the ϕ_1 arc is concentric with the $\lambda'_2\lambda'_3$ circle, ϕ_2 with $\lambda'_1\lambda'_3$ and ϕ_3 with $\lambda'_1\lambda'_2$ (Fig. 3b). The intersection of the three arcs defines L in Mohr space. Three angles ensure accuracy, but only two are necessary as shown in Mohr's original diagrams (Fig. 1) and in Fig. 3(b). For a fuller explanation of the construction, see Ramsay (1967, pp. 147–153).

Mohr diagrams are a useful means of illustrating and classifying strain ellipsoids of different types. The relationship of the ψ_{max} tangents to the three principal circles allows ellipsoids to be assigned to one of Ramsay's five equal-volume ellipsoid types (1967, pp. 154–158), by immediate inspection (Fig. 4). Using the popular k factor (Flinn 1962), where (in terms of λ) $k = [(\lambda_1/\lambda_2)^{1/2} - 1]/[(\lambda_2/\lambda_3)^{1/2} - 1]$, the $k = 1$ (plane strain, type 3) ellipsoids are immediately distinguishable

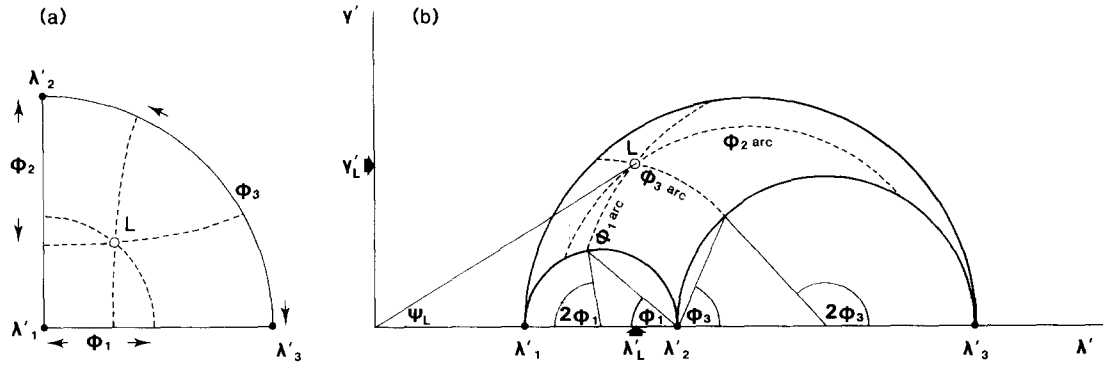

Fig. 3. The plotting of a point, L, on the Mohr diagram. (a) Quarter Lambert stereographic projection, illustrating angles ϕ_1, ϕ_2 and ϕ_3 of L to λ'_1, λ'_2 and λ'_3, respectively. (b) The three ϕ circular arcs which locate L and its coordinates λ'_L, γ'_L. L may be positioned from ϕ_1 and ϕ_3, only; note their single- and double-angle definitions. ψ_L is the angular shear for L.

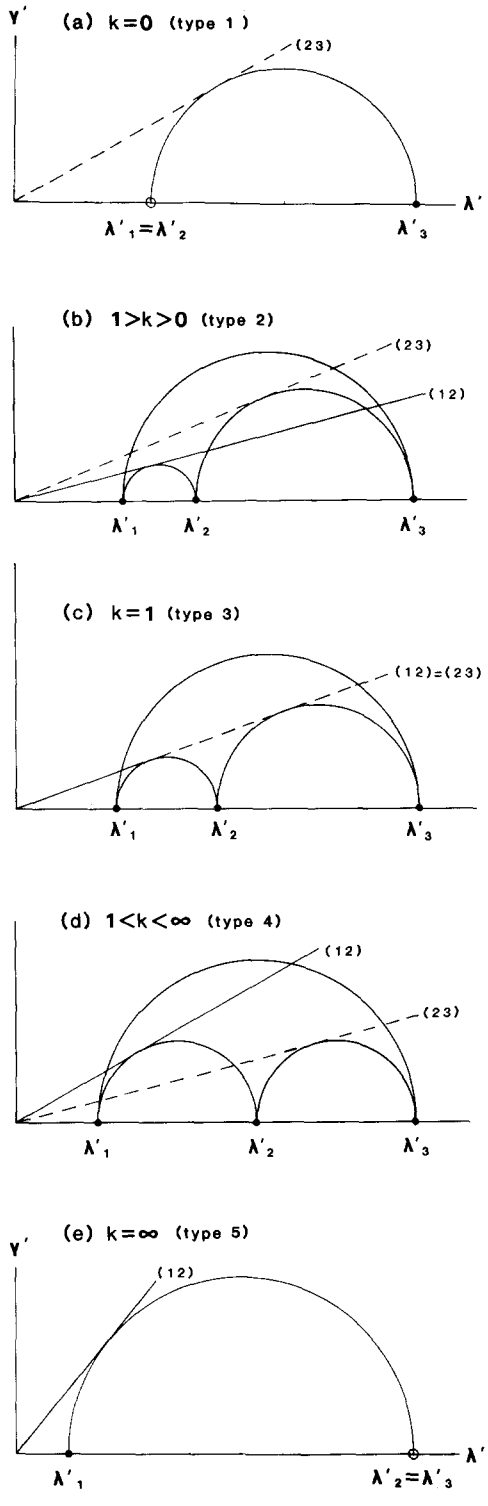

Fig. 4. Strain ellipsoid classification on the Mohr diagram. (a)–(e) are Ramsay's (1967) five ellipsoid types with k values as indicated. The ψ_{max} tangents to the $\lambda_1'\lambda_2'$ and $\lambda_2'\lambda_3'$ circles are shown by solid and broken lines, labelled (12) and (23), respectively. The relative disposition of these tangents allows immediate classification of any ellipsoid on a Mohr diagram.

(Fig. 4c): their $\lambda_1'\lambda_2'$ and $\lambda_2'\lambda_3'$ circles share the same ψ_{max} line. The two end-member ellipsoids, true prolate ($k = \infty$) and true oblate ($k = 0$) are represented on the Mohr diagram by a single Mohr circle (Figs. 4a & e): in each case, one principal circle reduces to a point and the other two are identical. The intensity of strain for each k class is represented by the different relative positions of λ_1',λ_2' and λ_3', given that $\lambda_1' \cdot \lambda_2' \cdot \lambda_3' = 1$.

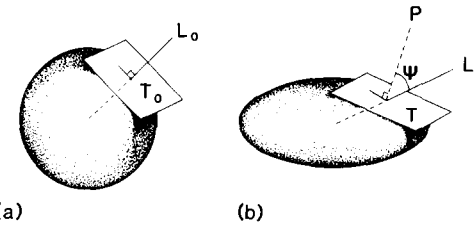

Fig. 5. Angular shear in three-dimensional strain. (a) The undeformed state represented as a sphere, with line L_0 as a radius and T_0 its perpendicular tangent plane. (b) In the deformed state the sphere becomes an ellipsoid, line L_0 deforms to L, and T_0 to ellipsoid tangent plane T, with pole P. Angular shear ψ for L is $\angle PL$.

Shear strain

The main distinction between the 2D and 3D Mohr diagrams is in the definition of shear strain, γ'. A Mohr circle represents the component of shear strain for a particular line, measured in a defined plane (the plane of the strain ellipse represented by the circle). On the 3D Mohr diagram the total shear strain is recorded.

In three-dimensional strain, the shear angle ψ for any line (e.g. L in Fig. 3) is defined as the angle between L and the pole to the deformed plane which was initially perpendicular to L (i.e. before deformation). It is most simply illustrated by considering the change from a sphere to an ellipsoid (Fig. 5). The line L is a deformed radius of the sphere, and the plane normal to L before strain (the tangent plane to the sphere), deforms to be the tangent plane to the ellipsoid. Thus ψ is the angle between the radius L and the pole to its tangent plane, P (Fig. 5), (Ramsay 1967 p. 128). For any direction (e.g. L in Fig. 3), ψ is measured simply on the Mohr diagram but its direction is not represented. Methods for determining the direction of ψ will be given in the following sections. These methods are not exactly equivalent to constructions for determining the direction of shear stress (e.g. Zizicas 1955, Jaeger & Cook 1969 p. 30, Johnson & Mellor 1973, p. 52) but share the same principle of resolving shear stress/strain into components.

The following analysis investigates the relationship between two-dimensional and three-dimensional strain, on the Mohr diagram. Mohr diagrams and Mohr circles will be used in conjunction, to represent sectional-ellipse planes of strain ellipsoids.

THE MOHR DIAGRAM TO REPRESENT SECTIONAL ELLIPSES —MOHR LOCI

The Mohr diagram represents lines in the strain ellipsoids by points, falling in the field bounded by the three principal-plane circles. Any plane section through a strain ellipsoid may thus be mapped by a series of points which represent a sheaf of lines in the plane. The configuration of points which defines any sectional-ellipse plane is here called a *Mohr locus*. Mohr loci have a variety of forms according to their orientation in the ellipsoid.

Three special Mohr loci are immediately obvious on

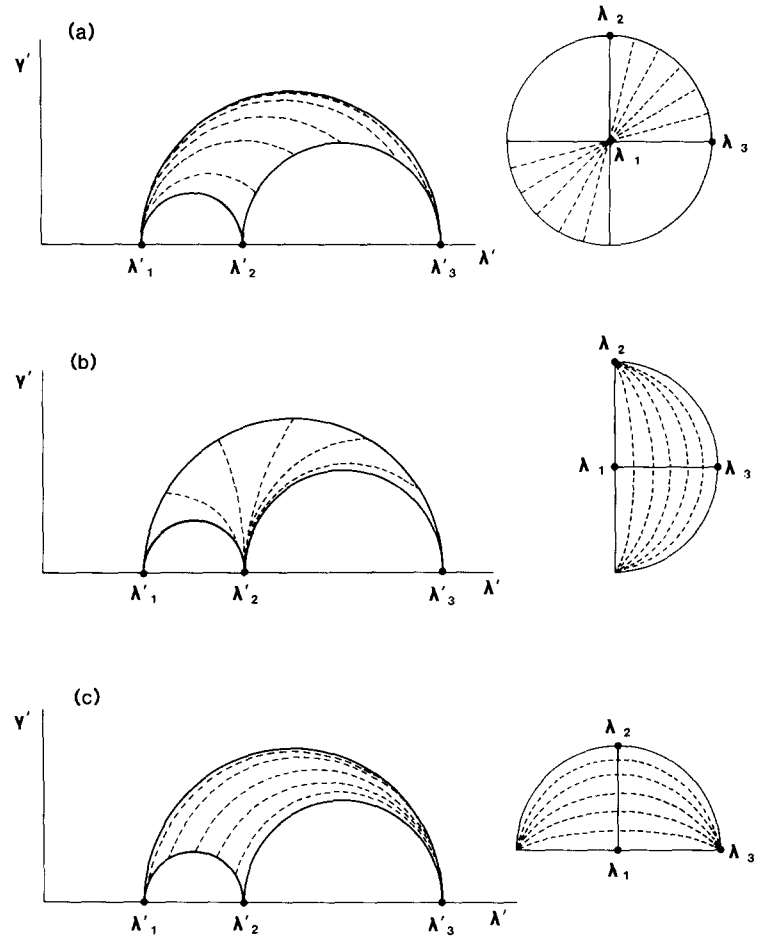

Fig. 6. The three forms of two-dimensionally oblique sectional ellipses on a Mohr diagram. The ellipse planes are represented stereographically on the right. In each, the ellipsoid principal planes are represented by solid lines, and sectional ellipse planes at 15° intervals by broken lines (circular arcs). (a) Planes parallel to λ_1, (b) parallel to λ_2 and (c) parallel to λ_3.

any Mohr diagram: these are the Mohr circles which represent the three principal planes of the ellipsoid. Sectional ellipses which contain one principal axis (two-dimensionally oblique) are also represented by circular arcs (Fig. 6). They are partial circles which meet in a point representing their common principal axis. A special Mohr locus of this type is the circular section or circular plane of the ellipsoid. For any ellipsoid, this is represented by the λ_2' ordinate (i.e. $\lambda' = \lambda_2'$) so, strictly, it is a partial circular arc of infinite radius (Fig. 7). In plane-strain ellipsoids ($k = 1$) (Fig. 7a) the circular-section locus represents the locus of lines of no finite longitudinal strain (n.f.l.s.): in all other cases ($k \neq 1$, Fig. 7b), the two loci do not coincide and the locus of n.f.l.s. represents a surface, not a plane (cf. Ramsay 1967, figs. 4.21 & 4.22).

The attitude of the circular section to λ_1' (angle θ) is determined by simple measurement on the Mohr diagram (Fig. 7) in either single or double-angle form. This is of practical use in the Biot–Fresnel construction (Gay 1967, p. 216). Moreover, it can be demonstrated from simple trigonometry in Fig. 7 that $\cos^2\theta = (\lambda_3' - \lambda_2')/(\lambda_3' - \lambda_1')$, and thus $\tan^2\theta = (\lambda_2' - \lambda_1')/(\lambda_3' - \lambda_2')$; see Flinn (1962), noting a difference in nomenclature. Flinn's $2V$ angle is supplementary to 2θ in Fig. 7.

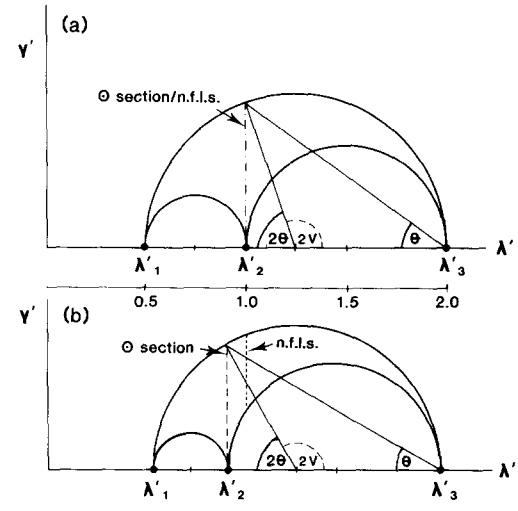

Fig. 7. The relationship of ellipsoid circular sections and surfaces of no finite longitudinal strain (n.f.l.s.). (a) In plane strain ($k = 1 = \lambda_2$) the two surfaces are the same; (b) in other cases ($k \neq 1$) they are different. θ is the angle of the two circular sections to λ_1, in single or double angle form, as used in the Biot–Fresnel construction. The $2V$ angle is also shown.

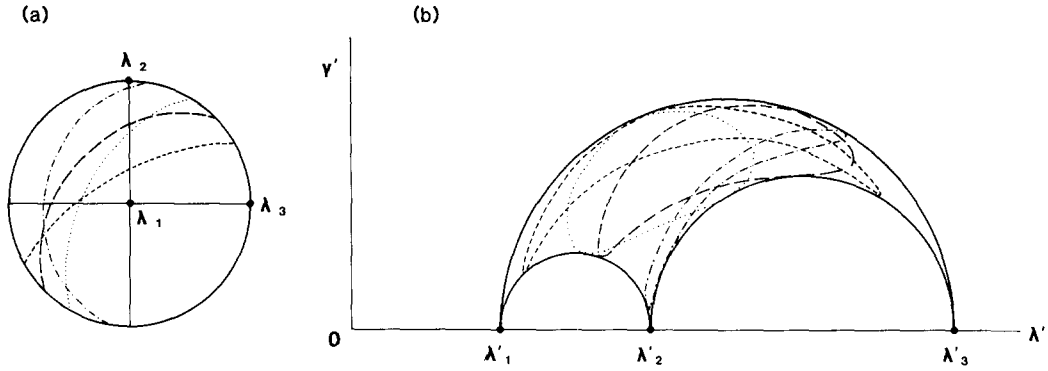

Fig. 8. Examples of the variation in shape of sectional ellipse loci. (a) Four three-dimensionally oblique sectional ellipse planes, in stereographic projection. (b) The Mohr loci for the four planes in (a). Note that each locus touches each principal circle once.

Mohr loci which represent section planes oblique to the three principal axes (3D-oblique) are not represented by circles or partial circles. They are closed forms of various shapes (oval, banana, etc.) according to their orientation in the ellipsoid (Fig. 8). Each Mohr locus touches the three principal circles once, where the sectional-ellipse plane intersects the principal planes in real space (A, B, C in Fig. 9). The exact shape of any locus is determined by careful plotting of a series of lines. The locus cannot be predicted (without algebra), but in practice it has proved possible to construct loci from an economical use of lines.

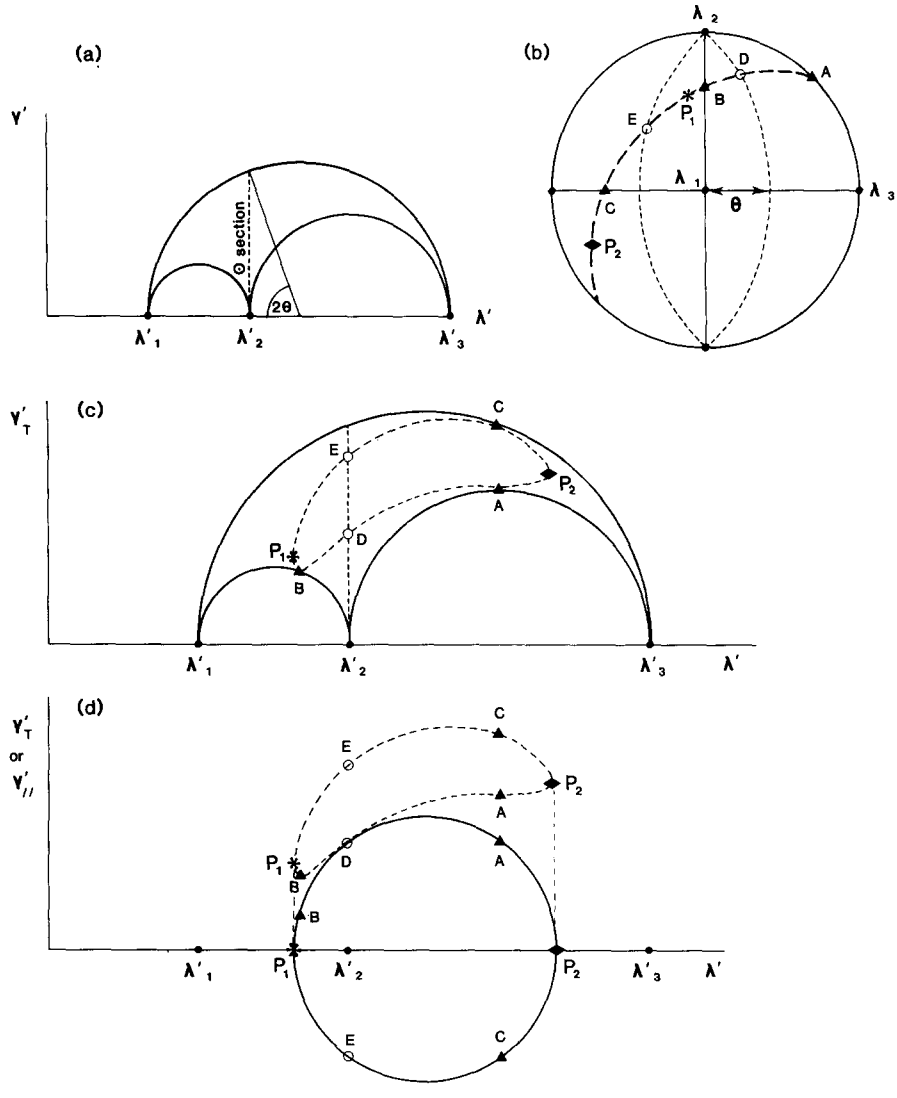

Fig. 9. Method of plotting sectional ellipses on the Mohr diagram for a known strain ellipsoid. A full explanation is given in the following text.

An economical method of Mohr-locus construction: Fig. 9

For a particular oblique section in the strain ellipsoid, a method is presented for its Mohr construction, to be read in conjunction with Fig. 9. It is assumed that the strain ellipsoid has a known axial ratio.

(a) Draw a three-circle Mohr diagram for the strain ellipsoid at an appropriate scale. Measure θ for the circular sections (cf. Fig. 7).

(b) Represent the strain ellipsoid orientation on a stereographic projection with λ_1 (X) vertical, λ_2 (Y) N–S and λ_3 (Z) E–W. Draw the great circle for the sectional ellipse in question (heavy broken curve). Label the principal-plane intersections A, B, C (triangles). Draw the two circular sections at angle θ to λ_1, intersecting in λ_2 (broken curves); label the intersections on the sectional-ellipse plane D, E (circles). Bisect angle $\angle$DE to obtain the two principal axes of the sectional ellipse, labelling P_1 the apparent extension (star) and P_2 the shortening (diamond). (This is the Biot–Fresnel construction: see, e.g. Gay 1967, p. 216.)

(c) Plot A, B and C on the principal Mohr circles by direct compass measurement. Plot D and E; one ϕ angle will locate each on the $\lambda' = \lambda_2'$ ordinate. Plot P_1 and P_2 by the circular-arc method described (see Fig. 3); two ϕ angles are necessary, three ensure accuracy. Construct a smooth locus through points A–E such that it touches the three principal circles once (A, B, C) and 'turns' at P_1 and P_2, the maximum and minimum λ' values (the extreme left and right points, respectively). Identify any particular section of uncertainty in the locus, and choose additional lines, as appropriate, constructing their positions from (b) to (c) as for P_1 and P_2.

(d) Construct the Mohr circle for the sectional ellipse, on principal axes P_1 and P_2. It should be tangent to the Mohr locus at one point. The relationship between Mohr loci and their circles is examined below.

The relationship between the Mohr locus and Mohr circle for a sectional ellipse

The locus of a sectional ellipse, constructed as described above, represents a graph of λ' vs γ' in three dimensions for the plane of the sectional ellipse. Any ellipse can be represented by a Mohr circle, the graph of λ' vs $\gamma_\parallel$, where $\gamma_\parallel$ here denotes the component of shear strain parallel to the plane of the sectional ellipse (Fig. 10a). For any line in the plane, $\gamma_\parallel$ is the shear strain of an initially perpendicular *line* in that plane, whereas γ_T is the shear strain of its initially perpendicular *plane*. The difference is worth emphasizing because shear strain is commonly described in two-dimensional terms (i.e. $\gamma_\parallel$) in structural-geology texts and also because the distinction between γ_T and $\gamma_\parallel$ is fundamental to the application of Mohr loci to structural problems described in this paper.

The relationship of the Mohr locus to the Mohr circle for a sectional ellipse is illustrated in Fig. 9 (d). The locus is transferred on ordinate tracks to become a circle with principal axes P_1 and P_2. This 'transfer' effectively removes the component of shear strain not parallel to the plane of the ellipse. All points on the locus (e.g. A, B, C) transfer to the circle, where their angular relationships are measurable in the usual Mohr-circle manner. The Mohr circle and Mohr locus touch at a single point which is the direction in the sectional ellipse where $\gamma_T = \gamma_\parallel$. (Coincidentally, in Fig. 9(d) this approximates to point D, a circular-section intersection.)

The ψ_T great circle for a sectional ellipse

The Mohr locus for a sectional ellipse plane, constructed as described above, is a graph of λ' vs total shear strain, γ_T', for the section. The direction of γ_T' for any line in the section plane is not represented on the Mohr diagram. The following construction allows the direction of γ_T' or ψ_T to be determined.

The values of two angular shear components are known from the Mohr locus and its Mohr circle, ψ_T and $\psi_\parallel$ (Fig. 10a). Consider the two ψ_T angles for the principal directions, P_1 and P_2, in the section plane. For these, $\psi_\parallel = 0$, which means that the angular shears for the tangent planes to P_1 and P_2 are measured perpendicular to the section plane (Fig. 10b). Their intersection N_o', locates the deformed initial normal to the section plane: this would be the relative position of a deformed initially perpendicular marker. Thus, $\angle NN_o'$ may be termed the polar shear, or $\psi_{\perp max}$ (Fig. 10c). The great circle perpendicular to N_o' is, here, called the ψ_T *great circle*. It allows the directions and values of ψ_T to be measured for any line in the section (Fig. 10c: points refer to Fig. 9), by a simple projection 'triangle' method. This, essentially, resolves the angular shear into three components which form a right-angled 'triangle' on the stereonet (Fig. 10d): $\psi_\parallel$ is measured (from the Mohr circle) on the net perimeter, $\psi_\perp$ on the net radius until it intersects the ψ_T great circle; the directions of ψ_T for each line are given by arrows on the 'triangle hypotenuse'.

The relationship between ψ_T, $\psi_\parallel$ and $\psi_\perp$ for any line has been expressed graphically in Fig. 10. In terms of algebra, the relationships are found to be

$$\cos\psi_T = \cos\psi_\parallel \cdot \cos\psi_\perp;$$
$$\gamma_T^2 = \gamma_\parallel^2 + \gamma_\perp^2 + \gamma_\parallel^2\,\gamma_\perp^2 \text{ and similarly for } \gamma';$$
$$\gamma_{\perp max}^2 = \gamma_{P1}^2 + \gamma_{P2}^2.$$

Two principles are illustrated in Fig. 10 which have practical implications. (i) The $\psi_\perp$ great circle may be constructed for any sectional ellipse from two ψ_T points: P_1 and P_2 are simplest in practice because their ψ_T directions are known. (ii) The ψ_T great circle can be constructed if the polar shear for the ellipse ($\psi_{\perp max}$) and its direction (Q) are known. These will define N_o', the pole to the ψ_T great-circle, thus allowing it to be drawn directly.

The ψ_T great circle, defined by either method, is the key to many practical applications of Mohr loci to geological problems. Taking the reverse procedure from the Mohr locus construction described previously (Fig. 9), it allows a locus to be constructed from a Mohr

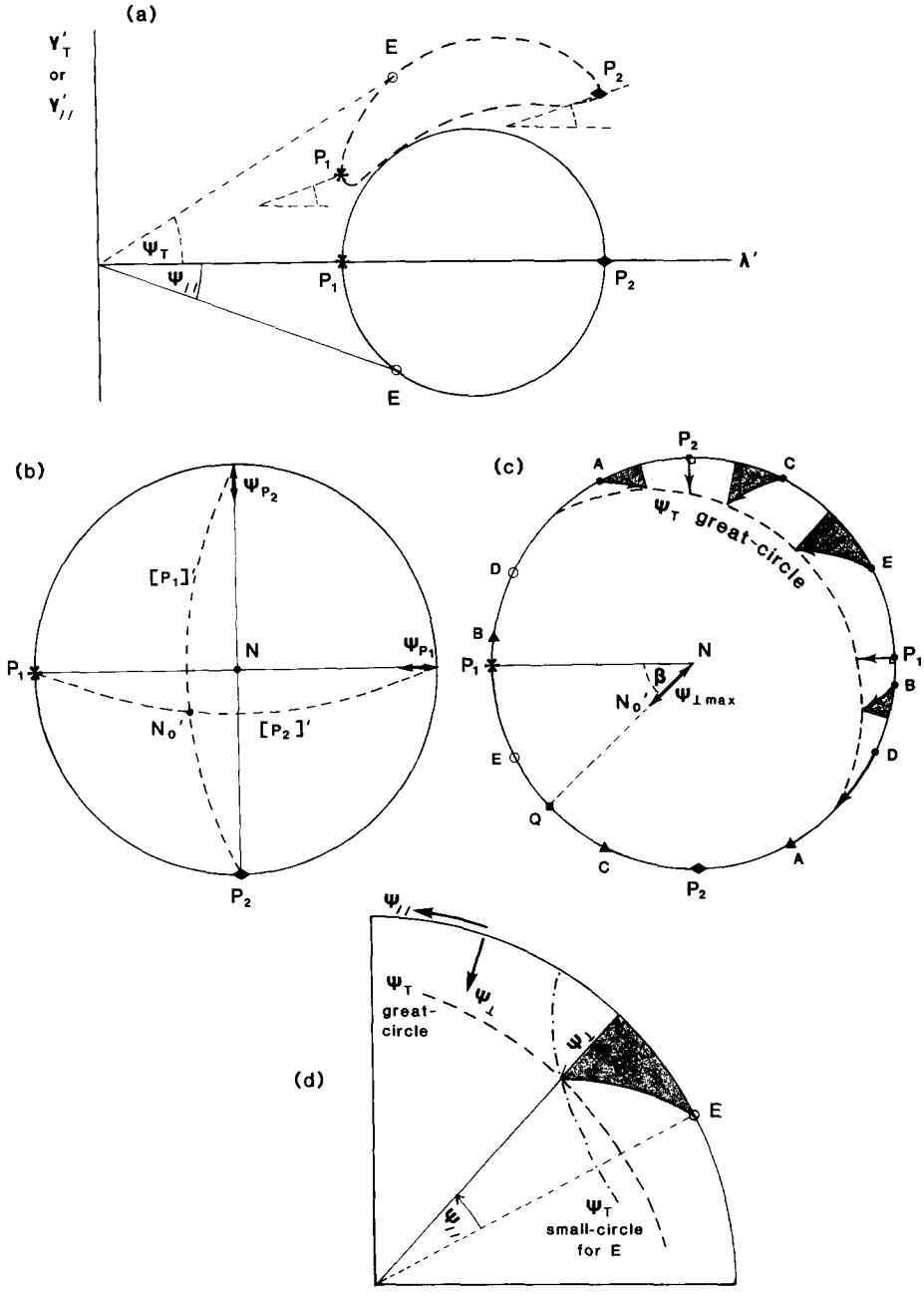

Fig. 10. (a) The Mohr locus and the Mohr circle from Fig. 9 showing angular shear components. Total angular shear ψ_T is measured from the locus (broken lines) and 2D (section-plane-parallel) shear, $\psi_{\|}$, from the Mohr circle (solid lines). (b) Angular shear for the two principal directions in the section plane, P_1 and P_2, as measured in (a). The Lambert stereographic projection shows the section plane horizontal. The 'deformed' tangent planes to P_1 and P_2 are broken curves, labelled $[P_1]'$ and $[P_2]'$: their intersection is the deformed original pole to the section plane, N_0'. (c) Angle $\angle NN_0'$ is $\psi_{\perp max}$, the polar shear in direction Q, at angle β to P_1. The great circle whose pole is N_0' is called the ψ_T great circle because it contains all ψ_T values for the section plane. 'Triangles' (shaded) may be constructed for each labelled point on the Mohr locus in Fig. 9. The perimeter side of any projection 'triangle' records $\psi_{\|}$, the perpendicular side the component called $\psi_{\perp}$, and the 'hypotenuse' represents the angle and direction of total shear, ψ_T (arrowed). (d) The 'triangle' for point E on a quarter projection, showing how the intersection of the $\psi_{\|}$ to $\psi_{\perp}$ trajectory with the ψ_T small circle falls on the ψ_T great circle for the section plane.

circle provided there is some data additional to the strain ellipse. Readers will already be familiar with the use of the Mohr circle for the derivation of a strain ellipse from particular types of two-dimensional data. Just as a single circle fits a particular set of data, a unique three-circle Mohr diagram for the strain ellipsoid can be fitted to a Mohr locus. The following practical examples illustrate some potential applications of Mohr loci to the derivation of strain ellipsoids in deformed rocks.

PRACTICAL APPLICATIONS OF MOHR DIAGRAMS AND LOCI IN GEOLOGICAL STRAIN MEASUREMENTS

Three examples are chosen to illustrate the potential of the Mohr diagram to the determination of three-dimensional strain. Each 'problem' is solved by completely graphical means—the combined use of stereographic projections and Mohr diagrams. Examples 1 and

3 are the situations treated algebraically in Ramsay (1967, pp. 142–149) and example 3 may also be solved by Owens' (1984) best-fit ellipsoid algorithm.

Clearly, graphical methods cannot compete with algebraic or numerical formulae, on accuracy. The choice of graphical vs accurate methods will depend on the need, and kind of data. Data determined by measurement are already limited in accuracy so the application of sophisticated numerical methods only produces a false sense of precision. In this situation a Mohr diagram solution would probably be more suitable: it requires no hardware/software, might even be used in the field, and with some practice is simple and quick. Probably the greatest advantage of the graphical solution is its physical representation of three-dimensional strain. By illustrating the strain ellipsoid on a plane, the Mohr diagram should remove the stumbling block which has forced many structural geologists to consider only two-dimensional problems.

Thus, it might be concluded that where exactness is not necessary, for single solutions or for a first approximation, the Mohr diagram is an ideal method of strain determination from geological data. While the answer may be inaccurate in some cases, the chance of deriving complete nonsense is remote.

Example 1: *a strain ellipse and a known orientation of ellipsoid axes*

This example is common in geology. A single (non-principal) strain ellipse may be measured or computed (e.g. from 'spots', fossils) and the principal axes of the strain ellipsoid may be inferred from cleavage ($\lambda_1\lambda_2$ or XY plane) and a stretching lineation in cleavage (λ_1 or X). The Mohr diagram is particularly suited to this problem. The key to the answer is the determination of the circular sections of the ellipsoid. The example also illustrates a case where single angles (Fig. 1a) are more useful than the usual double-angle Mohr convention.

For this example, a strain ellipse of axial ratio 1.5 has an orientation of ellipsoid axes (λ_1, λ_2, λ_3) as shown in Fig. 11(a). Following the earlier formulation, the principal axes are labelled P_1, P_2 and the principal-plane intersections A, B, C. Using the Biot–Fresnel construction in reverse, a pair of circular sections may be constructed (to intersect at λ_2) by trial-and-error. Only one pair exists for which P_1 and P_2 are the bisectors of the two circular-section intersections on the ellipse plane (D, E) (Fig. 11b). The construction of these planes is the step to an easy solution.

The next stage is to draw the Mohr circle (on a relative

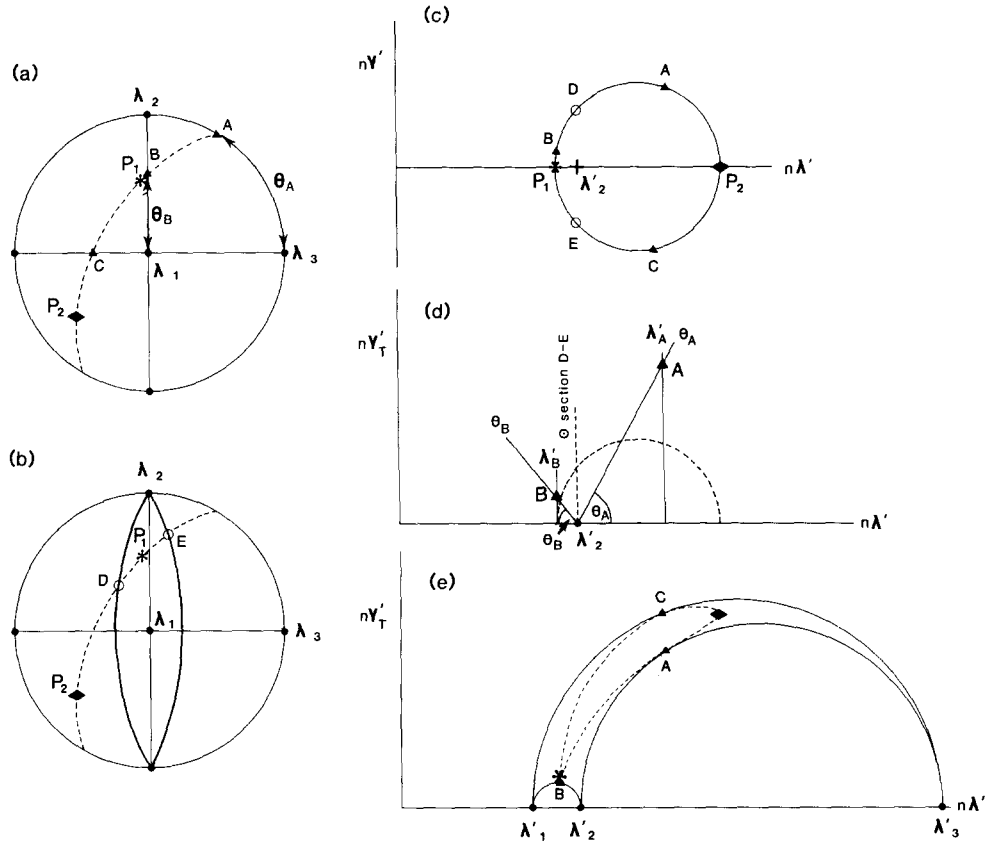

Fig. 11. Example 1: a strain ellipse with axial ratio 1.5 and known orientation of ellipsoid principal axes. (a) Stereographic representation of the known ellipse, its principal axes P_1 (relative extension) and P_2 (relative shortening) and the principal plane intersections A, B, C, (symbols as Fig. 9). Angle $\angle A\lambda_3$ is labelled θ_A; $\angle B\lambda_1$ θ_B. (b) Trial-and-error construction of the two circular sections (solid) for which P_1 and P_2 bisect intercept D–E (circles) in the sectional ellipse plane (reverse Biot–Fresnel construction: see also De Paor 1986). (c) Construction of the Mohr circle for the ellipse on a relative scale ($n\lambda'$, $n\gamma'$): axial ratio $R = 1.5$ (i.e. $\lambda_{P_1}/\lambda_{P_2} = 2$). Points A–E are shown. The ordinate through D–E locates λ_2' (cross). (d) Angles θ_A and θ_B constructed by the single-angle convention (cf. Figs. 1a and 3b). The intersections of the θ_A and θ_B chords with the λ_A' and λ_B' ordinates (given in c) locate A and B in the 3D Mohr diagram (triangles). (e) The Mohr diagram for the strain ellipsoid satisfying the data. The $\lambda_1'\lambda_2'$ circle is drawn through B and λ_2', and the $\lambda_2'\lambda_3'$ circle through A and λ_2'. The Mohr locus for the sectional ellipse in (c) is sketched approximately, for completeness.

scale) for the strain ellipse (Fig. 11c), and plot points A–E in the usual way. (Note that their positions represent their λ' values but their ordinate values are $\gamma'_{\|}$ not γ'_{T}). Points D and E are important: they fall on the ordinate line which represents the circular sections, and thus determines λ'_2. λ'_2 is now known: it remains to locate λ'_1 and λ'_3. Recall the single-angle Mohr circle convention (Figs. 1a and 3b) where angles to a principal axis are measured on chords from the diametrically opposite axis. Two angles may be measured on chords from λ'_2: θ_A, the angle $\angle A\lambda'_3$ on the $\lambda'_2\lambda'_3$ circle and θ_B, the angle $\angle B\lambda'_1$ on the $\lambda'_1\lambda'_2$ circle, labelled in Fig. 11(a). These chords are constructed in Fig. 11(d). The intersection of the θ_A chord with the A ordinate (given on the Mohr circle, Fig. 11c) locates A on the (3D) Mohr diagram. B is located likewise.

The position of A, together with λ'_2, allows the $\lambda'_2\lambda'_3$ principal circle to be drawn. The $\lambda'_1\lambda'_2$ circle is similarly constructed through λ'_2 and B. The $\lambda'_1\lambda'_3$ circle is now obvious, and the three-circle Mohr diagram for the strain ellipsoid complete (Fig. 11e). Absolute values may be given to λ'_1, λ'_2 and λ'_3 from the relative scale in Fig. 11(e) if equal volume ($\lambda'_1 \cdot \lambda'_2 \cdot \lambda'_3 = 1$) is assumed. The present example reveals a strain ellipsoid with $X = 1.37$, $Y = 1.14$ and $Z = 0.64$. ($X = \lambda_1'^{-1/2}$, $Y = \lambda_2'^{-1/2}$, $Z = \lambda_3'^{-1/2}$).

The solution in this example, unlike the following two, is not dependent on the construction of a Mohr locus for the strain ellipse. However, the locus is shown approximately in Fig. 11(e) for completeness.

Example 2: a bedding-plane strain ellipse and bedding-normal shear strain

This is the situation in which a strain ellipse can be measured or computed on a bedding plane and the angular shear normal to bedding is measurable. For example, there may be distorted fossils on a bedding plane and deformed burrows or worm tubes initially normal to bedding. In terms of the preceding account, the data is thus a bedding plane sectional ellipse (Mohr circle) and its polar shear value, $\psi_{\perp max}$, and direction (Q) (cf. Fig. 10). The data are insensitive to bedding compaction strain, assumed to be zero in this example.

The present example considers the case of a strain ellipse with axial ratio 1.5, and polar shear $\psi_{\perp max} = 20°$ at 30° to the principal ellipse extension, P_1. The method is as follows. First draw the Mohr circle for the ellipse on a relative scale (Fig. 12a) marking the polar shear direc-

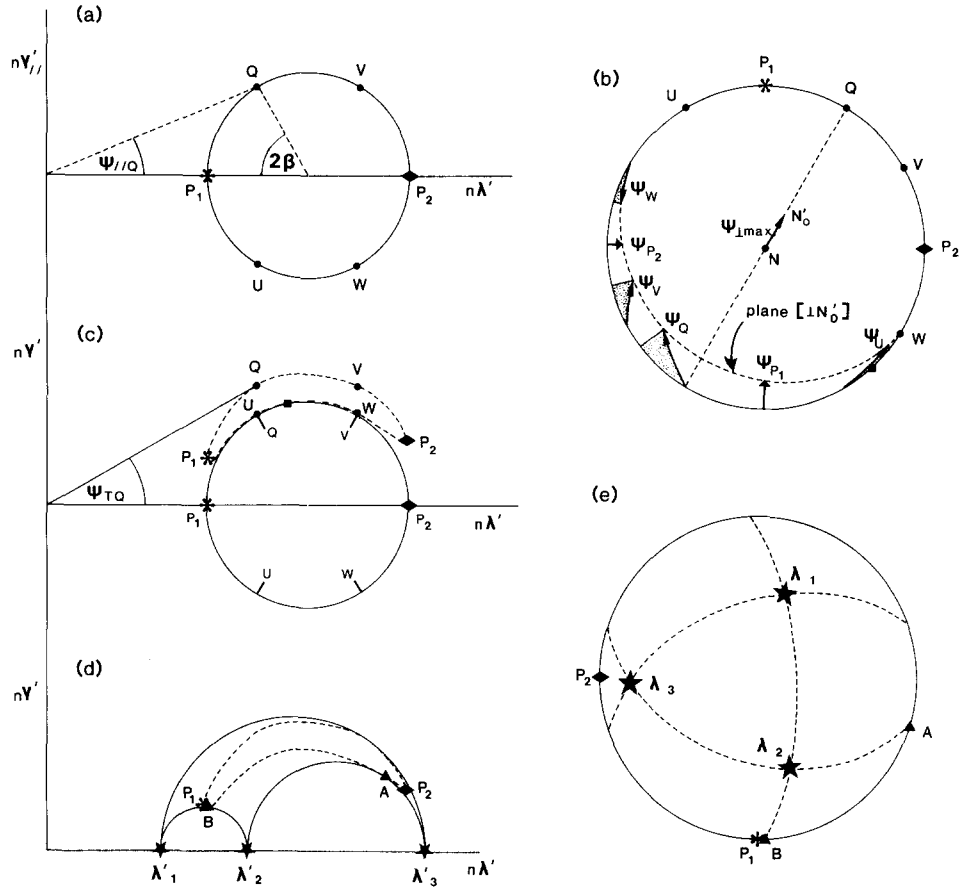

Fig. 12. Example 2: a bedding plane strain ellipse of axial ratio 1.5 and a polar shear strain of 20° at 30° to the ellipse extension. (a) The Mohr circle for the strain ellipse on a relative scale. Q is the azimuth of the polar shear strain ($\beta = 30°$). $\psi_{\|}$ is measured for Q and other selected points (U, V, W). (b) Stereographic representation of the strain ellipse (horizontal), following Fig. 10. The polar shear ($\psi_{\perp max}$) determines N'_o (the deformed initial pole to the ellipse plane) which is the pole to the ψ_T plane. ψ 'triangles' are constructed for Q, U, V, W from their $\psi_{\|}$ values in (a); arrowheads denote the values and orientations of ψ_T for each, to be plotted in (c). (c) Construction of the points on the Mohr diagram and their relationship to the Mohr circle. The Mohr locus is drawn (broken crescent). (d) Three principal Mohr circles are fitted to the Mohr locus, each one touching the locus once. Two principal intersections (A, B) are used to construct the orientation of λ_1, λ_2 and λ_3 (stars) in (e) with respect to the (horizontal) sectional ellipse.

tion Q. Measure the ellipse-parallel shear component ($\psi_{\parallel}$) for Q, from the Mohr circle. Now, represent the ellipse stereographically, as the horizontal plane. $\psi_{\perp max}$ is represented by the angle $\angle NN'_o$, azimuth Q. The plane perpendicular to N'_o is the ψ_T locus plane: this will be used, together with the $\psi_{\parallel}$ values measured in (a) (e.g. Q) to determine ψ_T values, as shown in Fig. 10. The ψ_T values for a series of points on the ellipse plane will allow the Mohr locus to be constructed. Figure 12(b) shows the ψ_T values for selected lines: P_1 and P_2 where $\psi_{\parallel} = 0$; Q, T, U and V (chosen), by the projection 'triangle' method described previously. The ψ_T angles are carefully measured in Fig. 12(b) and transferred to a Mohr diagram (Fig. 12c). Six points on the Mohr locus are thus determined; more may be constructed if necessary. The Mohr locus for the sectional ellipse is smoothly drawn through these points (Fig. 12c). It must touch its Mohr circle at a single point, and be such that P_1 is its most leftward point and P_2 its most rightward.

In a perfect example, there is only one set of principal Mohr circles (on $\lambda'_1, \lambda'_2, \lambda'_3$) which will completely enclose the Mohr locus. In practice, this is found by trial-and-error which may require finding the best imperfect fit (Fig. 12d). Each circle should touch the locus once (A, B, C); these three principal-plane intersections allow the orientation of the principal axes to be determined, and constructed (Fig. 12e); (refer back to Fig. 9).

The strain ellipsoid and its orientation to the bedding-plane ellipse are thus derived, entirely graphically. As for example 1, values may be given to X, Y and Z assuming an equal-volume strain ellipsoid. In the present example $X = 1.34$, $Y = 1.01$ and $Z = 0.74$.

Example 3: three sectional strain ellipses

This last example is chosen because it is a common geological situation, and one for which algebraic or numerical methods are generally used (Ramsay 1967, pp. 142–148, Milton 1980, Ramsay & Huber 1983, p. 198, Owens 1984). The method described below is entirely graphical, as also is De Paor's (1986) method by orthographic projection.

The geological data is in the form of three strain ellipses of known axial ratio and orientation, on three planes of known mutual orientation. These strain ellipses may have been derived by direct measurement on bedding/joint planes in the field, measured on sectioned rock specimens or computed on section planes by methods such as Fry's (1979). The three section planes will be called xy, yz and xz where x, y and z are their mutual intersections, the section axes. The present example considers the case of three mutually perpendicular section planes, but the method is applicable to any three section planes.

Represent the three sectional ellipse planes stereographically (Fig. 13a) labelling the principal extensions, P_1, and shortenings, P_2. It is convenient to construct one section plane horizontally with a section axis N–S; the other planes are then oriented accordingly. In this example xz is the horizontal plane and xy and yz are vertical. Construct the Mohr circles for the three sectional ellipses on any suitable scale (Fig. 13b), and mark the section axes x, y, z on each; they are diagonals in this orthogonal case. The example in Fig. 13 has ellipse strain ratios of 1.38, 1.85 and 1.37 on the xy, yz and xz planes, respectively. The three Mohr circles in Fig. 13(b) can only be used for angular measurements, because their absolute scales are not represented. It is possible, by altering the scaling of each circle, to construct the three circles on the same scale, such that λ'_x is the same for x on the xy and xz circles, (similarly λ'_y and λ'_z) (Fig. 13c). However, this is laborious and not necessary for the final solution.

On each Mohr circle in Fig. 13 (b), measure two values of angular shear ($\psi_{\parallel}$) for the x, y and z axes. The nomenclature is given as such: $\psi_{x(xy)}$ refers to the angular shear for x parallel to the xy plane. The six measured angles are $\psi_{x(xy)}$, $\psi_{y(xy)}$, $\psi_{y(yz)}$, $\psi_{z(yz)}$, $\psi_{x(xz)}$ and $\psi_{z(xz)}$. Their significance is shown in Fig. 13(d) and their values allow three planes to be drawn which represent the strain ellipsoid tangent planes at x, y and z. The tangent plane for x is labelled $[\perp x]'$ (i.e. the deformed plane originally perpendicular to x); the total angular shear for x (ψ_x) is given by the angle between x and the pole to $[\perp x]'$ (see Fig. 5). The total angular shears for x, y and z are thus derived, arrowed in Fig. 13(d).

The three values for total shear (ψ_T) for x, y and z provide sufficient data for constructing a ψ_T great-circle for each (or all) of the sectional-ellipse planes. The ψ_T plane is drawn in Fig. 13(e) for the xz (horizontal) plane, through the ψ_x and ψ_z arrowheads. Recall that a ψ_T plane provides the data for converting a Mohr circle to a Mohr locus on the (3D) Mohr diagram (see Fig. 10 and example 2). Figure 13(f) shows a series of Mohr locus points transferred from their xz Mohr circle positions, according to their values of ψ_T derived in Fig. 13(e). Points x, z, P_1 and P_2 can be simply located, but certain additional points (T, U, V, W) must be selected and ψ triangles (shaded in Fig. 13e) constructed as described previously. A Mohr locus is constructed for the xz sectional ellipse through the eight points in Fig. 13(f); see earlier discussion of Mohr loci construction, and number of points needed.

There should only be one set of principal Mohr circles (defining the strain ellipsoid) which can be fitted to an accurate Mohr locus. In practice, a best-fit ellipsoid must be sought for the xz locus in Fig. 13(f); this is constructed in Fig. 13 (g). On the assumption $\lambda'_1 \cdot \lambda'_2 \cdot \lambda'_3 = 1$, the strain ellipsoid in Fig. 13(g) has axial ratios $X = 1.4$, $Y = 1$ and $Z = 0.7$. The three tangent points of the Mohr locus to the principal circles (A, B and C) allow the orientations of λ_1, λ_2 and λ_3 (X, Y, Z) to be constructed with respect to the xz plane, as described previously. The solution is shown in Fig. 13 (h).

A solution for the strain ellipsoid fitting the strain data on three section planes could have been derived from the Mohr locus construction of each of the section planes. Ideally, the ellipsoid should be the same although the shape of each locus will be different. In

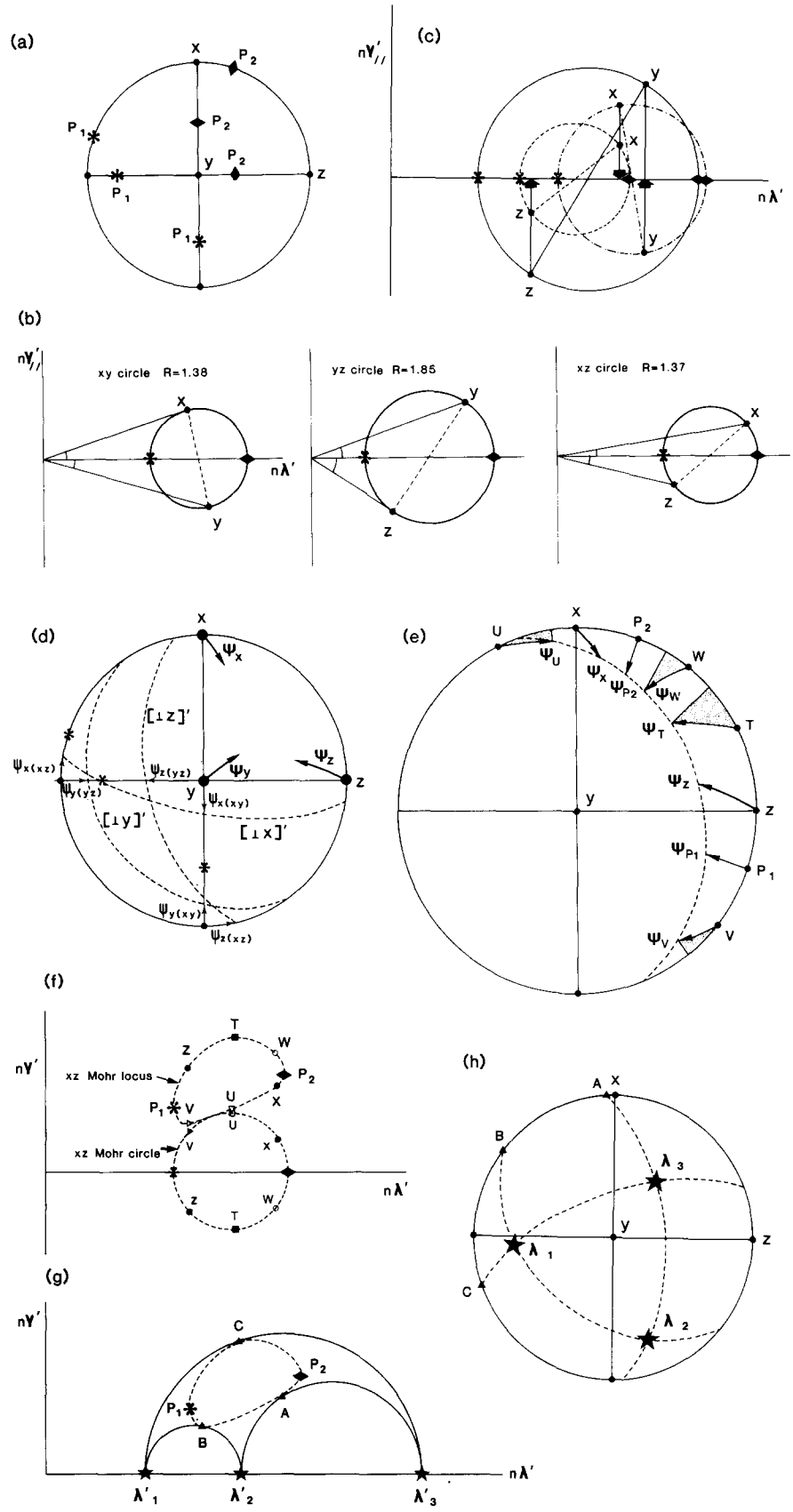

Fig. 13. Example 3: strain measurement on three mutually perpendicular planes. (a) Three sectional ellipse planes xy, yz and xz, their section axes x, y and z and their principal elongations (P_1) and shortenings (P_2). (b) The three Mohr circles and six shear angles: scale unimportant. (c) The three Mohr circles constructed on a compatible relative scale so that their λ'_x, λ'_y and λ'_z values are in common (arrowed). This diagram is not necessary to the solution. (d) The six shear angles measured in (b) represented on a stereographic construction. They allow the ellipsoid tangent planes to x, y and z to be constructed ($[\perp x]'$, etc.) and thus the total shear angles for x, y and z to be represented (heavy arrows: ψ_x, ψ_y and ψ_z). (e) For the horizontal xz plane the ψ_T great circle is constructed from ψ_x and ψ_z (cf. Fig. 10). (f) The xz Mohr circle is drawn, a series of points defined (T, U, V, W), and their $\psi_{\parallel}$ angles measured. Their ψ_T angles are determined from the construction of 'triangles' in (e). Each ψ_T value (arrowed) is plotted on the Mohr diagram, (f), to construct the xz Mohr locus. (g) As in example 2, three principal Mohr circles are fitted to the locus. Tangent points A, B, C, allow λ_1, λ_2 and λ_3 (stars) to be constructed relative to x, y and z, in (h).

practice, three ellipse sections might not fit one common ellipsoid: see De Paor (1986) for a discussion of closing errors.

This final example demonstrates the potential of the Mohr diagram, and particularly the power of Mohr loci, for the derivation of strain ellipsoids from data hitherto analysed algebraically or by computer. Although less accurate than these, the Mohr diagram provides an entirely graphical method which is straightforward, immediate and cheap; it is particularly suited for a 'first try' of data. A direction for future research might be in minimizing the element of human error inherent in graph drawing and angle measurement by using a computer to construct Mohr diagrams, Mohr loci and stereographic projections. The visual advantages of the Mohr diagram would thus be combined with the greater exactness of computer methods.

CONCLUSIONS

An investigation of the Mohr diagram for three-dimensional strain has revealed considerable potential to structural geology. A three-circle Mohr diagram for a strain ellipsoid provides a simple immediate method of ellipsoid classification according to its k type. However, the area of greatest potential is probably in the representation of sectional ellipses as Mohr loci. These loci provide a link between two-dimensional strain of Mohr circles and the three-dimensional Mohr diagram. The selected examples illustrate the power of the Mohr diagram and Mohr loci to solving problems of three-dimensional strain by graphical means.

Acknowledgements—I should like to thank the Department of Geology, University of Manchester for an Honorary Fellowship which enabled me to undertake this work. Thanks go to Catherine Hardy for typing the manuscript, Phil Stubley for drafting the figures and Jack Treagus for interest and advice. I particularly wish to acknowledge correspondence with Declan De Paor which helped to clarify some aspects of three-dimensional shear strain and the Mohr diagram at an early stage of the work. His suggestions and those of an anonymous reviewer are much appreciated.

REFERENCES

Allison, I. 1984. The pole of the Mohr diagram. *J. Struct. Geol.* **6**, 331–333.

Brace, W. F. 1961. Mohr construction in the analysis of large geologic strain. *Bull. geol. Soc. Am.* **72**, 1059–1080.

Cutler, J. & Elliott, D. 1983. The compatibility equations and the pole to the Mohr circle. *J. Struct. Geol.* **5**, 287–297.

De Paor, D. G. 1983. Orthographic analysis of geological structures—I. Deformation theory. *J. Struct. Geol.* **5**, 255–277.

De Paor, D. G. 1986. Orthographic analysis of geological structures—II. Practical applications. *J. Struct. Geol.* **8**, 87–100.

De Paor, D. G. & Means, W. D. 1984. Mohr circles of the First and Second Kind and their use to represent tensor operations. *J. Struct. Geol.* **6**, 693–701.

Flinn, D. 1962. On folding during three-dimensional progressive deformation. *Q. Jl geol. Soc. Lond.* **118**, 385–433.

Fry, N. 1979. Random point distributions and strain measurement in rocks. *Tectonophysics* **60**, 89–105.

Gay, P. 1967. *An Introduction to Crystal Optics*. Longmans, Green, London.

Jaeger, J. C. 1956. *Elasticity, Fracture and Flow*. Methuen, London.

Jaeger, J. C. & Cook, N. G. W. 1969. *Fundamentals of Rock Mechanics*. Chapman & Hall, London.

Johnson, W. & Mellor, P. B. 1973. *Engineering Plasticity*. Van Nostrand Reinhold, London.

Means, W. D. 1982. An unfamiliar Mohr construction for finite strain. *Tectonophysics* **89**, T1–T6.

Means, W. D. 1983. Application of the Mohr-circle construction to problems of inhomogeneous deformation. *J. Struct. Geol.* **5**, 279–286.

Milton, N. J. 1980. Determination of the strain ellipsoid from measurements on any three sections. *Tectonophysics* **64**, T19–T27.

Mohr, O. 1982. Ueber die Darstellung des Spannungszustandes und des Deformationszustandes eines Körperelementes und über die Anwendung derselben in der Festigkeitslehre. *Civilingenieur* **28**, 113–115.

Mohr, O. 1900. Welche Umstände bedingen die Elastizitatsgrenze und den Bruch eines Materiales? *Zeitschrift des Vereimes deutscher Ingenieuse* **44**, 1524–1530.

Mohr, O. 1905. *Abhandlungen aus dem Gebiete der Technischen Mechanik*. Ernst & Sohn, Berlin.

Nadai, A. 1931. *Plasticity*. McGraw-Hill, New York.

Nadai, A. 1950. *Theory of Flow and Fracture of Solids*. McGraw-Hill, New York.

Owens, W. H. 1984. The calculation of a best-fit ellipsoid from elliptical sections on arbitrarily oriented planes. *J. Struct. Geol.* **6**, 571–578.

Ramsay, J. G. 1967. *Folding and Fracturing of Rocks*. McGraw-Hill, New York.

Ramsay, J. G. & Huber, M. I. 1983. *The Techniques of Modern Structural Geology. Volume 1: Strain Analysis*. Academic Press, London.

Treagus, S. H. 1983. A theory of finite strain variation through contrasting layers, and its bearing on cleavage refraction. *J. Struct. Geol.* **5**, 351–368.

Zizicas, G. A. 1955. Representation of three-dimensional stress distribution by Mohr circles. *J. appl. Mech.* **22**, 273–275.